Nonlinear displacement-based response prediction of reinforced concrete columns

H. Mostafaei [a,*], F.J. Vecchio [a], T. Kabeyasawa [b]

[a] *Department of Civil Engineering, University of Toronto, 35 St. George Street, M5S 1A4, Toronto, Canada*
[b] *Earthquake Research Institute, The University of Tokyo, Tokyo 113-0032, Japan*

Abstract

In this study, the application of two nonlinear finite element method (FEM) procedures and a simplified axial-shear-flexure interaction approach are examined for displacement-based analysis of four reinforced concrete columns, previously tested. The two alternative finite element methods are described based on differing crack modeling approaches: smeared rotating cracks, implemented by the VecTor2 program, and smeared fixed cracks, implemented by the UC-win/WCOMD program. The Axial-Shear-Flexure Interaction approach, a method also based on smeared rotating cracks, is simplified, discussed and compared with the FEM analyses. Experimental and analytical results are compared for pre- and post-peak responses up to axial collapse of the columns. Both FEM methods resulted in satisfactory pre-peak predictions. Adequate post-peak simulations, until near complete loss of capacity, were achievable by the rotating crack method (VecTor2), especially for those columns exhibiting a shear-critical response. The simplified Axial-Shear-Flexure Interaction approach provided response envelope curves for the specimens comparable with the cyclic results obtained by the two FEM approaches.
© 2008 Elsevier Ltd. All rights reserved.

Keywords: Finite element models; Reinforced concrete; Section analysis; Rotating and fixed cracks; Shear-flexure interaction; Columns; Nonlinear analysis

0. Introduction

In the past four decades, several analytical approaches and finite element models has been developed to simulate the behavior of reinforced concrete structures subjected to various loading conditions. Until recently, structural design approaches were mainly based on load and capacity evaluation concepts. However, reconnaissance and experimental studies on structural performance conclusively showed that a comprehensive design cannot be achieved by a capacity-based methodology. Hence, performance-based or displacement-based evaluation approaches emerged into the field of design engineering and practice. One of the well-known and widely-used displacement-based analytical approaches for reinforced concrete structures is the smeared crack and average stress–strain concept. This methodology can be subdivided into fixed smeared crack [1] and rotating smeared crack [2] approaches. In the former method, once a crack is generated,

its direction is considered geometrically fixed. However, in the latter method, crack directions rotate together with the principal stress and strain vectors. The main hypothesis of the smeared rotating crack approach is that both principal stress and strain vectors are assumed coincident in the process of analysis. In the fixed crack concept, no restriction is imposed on the concrete stress and strain fields to be coincident.

Here, an attempt is made to assess the reliability of the above two methods for displacement-based analysis of reinforced concrete columns. The authors selected two well-known available programs for this study: VecTor2, developed at University of Toronto based on the smeared rotating crack approach, and WCOMD, developed at University of Tokyo based on the fixed smeared crack method. As an alternative macro-model method, the Axial-Shear-Flexure Interaction (ASFI) method [3,9], developed based on the smeared rotating crack approach, is also examined in this study for further simplification and implementation.

For experimental corroboration, four reinforced concrete column specimens with different failure modes of shear, shear-compression, and flexure, loaded under constant axial load and

---

* Corresponding author. Fax: +1 416 929 7436.
E-mail address: h.mostafaei@utoronto.ca (H. Mostafaei).

Notations

B	width of the section
C_d	a factor, defined in terms of concrete tensile and compression strains
C_s	a factor that accounts for the influence of slippage on the cracks.
d	effective depth of the section
d_f	flexure depth of the section
d_s	shear depth of the section.
f_c'	concrete compression strength
f_{cx}	concrete stress in x-direction
f_{cy}	concrete stress in y-direction
f_{sx}	average reinforcement stress in x-direction
f_{sy}	average reinforcement stress in y-direction
f_t'	concrete tensile strength
H	depth of the section
ℓ_{12}	the distance between two adjacent flexural sections
L_{in}	distance between the flexure section and the inflection point
m	a factor in terms of the reinforcement ratio and the rebar diameter
M	moment at the flexure section
P	applied axial load
V	applied lateral load
v_{cxy}, v_{cyx}	concrete shear stress relative to x and y axes
β	compression softening factor
ε_x	average strain in x direction, and for columns, it is the total axial strain
ε_y	average strain in y direction
ε_{xa}	axial strains due to axial mechanism
ε_{xs}	axial strains due to shear mechanism
ε_{xf}	axial strains due to flexural mechanism
ε_{sx}	strain of the reinforcement parallel to the x direction
ε_{sy}	strain of the reinforcement parallel to y direction
ε_{cx}	concrete strain in x direction
ε_{cy}	concrete strain in y direction
ε_{xc1} and ε_{xc2}	the centroidal strains of two adjacent flexural sections
$\{\varepsilon\}_{c0}$	uncracked concrete strain vector for the WCOMD
$\{\varepsilon\}_{ci}$	strain due to crack in the i direction for the WCOMD
γ	total lateral drift of a column between two flexure sections
γ_s	shear strain
γ_f	flexural drift ratio
ρ_{sx} and ρ_{sy}	reinforcement ratios in the x and y directions
σ_o	applied axial stress
σ_x	total stress in x direction
σ_y	total stress in y direction
σ_{xf}	axial stress in the axial-flexure element
σ_{xs}	axial stress in the axial-shear model
σ_y and σ_z	stresses in the axes perpendicular to the axial axis of a column, or clamping stresses

$\{\sigma\}_{rc}, \{\sigma\}_c$, and $\{\sigma\}_r$	stress vectors in the reinforced concrete, cracked concrete and reinforcement for the WCOMD
τ	resultant shear stress
τ_f	shear stress in the axial-flexure element
τ_s	shear stress in the axial-shear model
τ_{xy}	shear stress

cyclic lateral load [4] are modelled to examine and verify the analytical results.

1. VecTor2 and the smeared rotating crack concept

VecTor2 is a program based on the Disturbed Stress Field Model [10–12], a refinement of the Modified Compression Field Theory [5] for nonlinear static and dynamic finite element analysis of reinforced concrete membrane structures. It is supported by the FormWorks program as a pre-processor for structural configuration, and by the Augustus program as a post-processor for visualizing the results of VecTor2. Here a brief description of the Modified Compression Field Theory (MCFT) is presented. Additional detail can be found in [10–12].

1.1. MCFT stress–strain model

The MCFT is based on formulations of principal average strains in an element leading to the calculation of principal average stresses in concrete through realistic nonlinear constitutive relationships. Transforming average concrete principal stresses to global coordinate axes and adding in average steel bar stresses gives the total average stresses in the element. There are two checks in the calculation process relating to crack zones. The first is to ensure that tension in concrete can be transferred across the crack. The second is to ensure that shear stress on the surface of the crack dose not exceed the maximum shear resistance provided by aggregate interlock. A reinforced concrete element, in the Modified Compression Field Theory, can be illustrated as the free body diagram of the membrane element depicted in Fig. 1.

1.2. Compatibility and equilibrium conditions

Assuming a perfect bond, compatibility relationships in the MCFT are expressed by the following equations based on average strains in concrete and reinforcement:

$$\varepsilon_x = \varepsilon_{cx} = \varepsilon_{sx} \tag{1}$$

$$\varepsilon_y = \varepsilon_{cy} = \varepsilon_{sy} \tag{2}$$

where ε_x, ε_y are average strains in x and y directions, shown in Fig. 2, ε_{sx}, ε_{sy} are strains of the reinforcement parallel with the x and y directions respectively, and ε_{cx}, ε_{cy} are concrete strains in x and y directions: [Note: in the general form of the MCFT, any number of reinforcement components can exist, and can be oriented in arbitrary directions.] For an in-plane shear element, shown in Fig. 3, equilibrium conditions
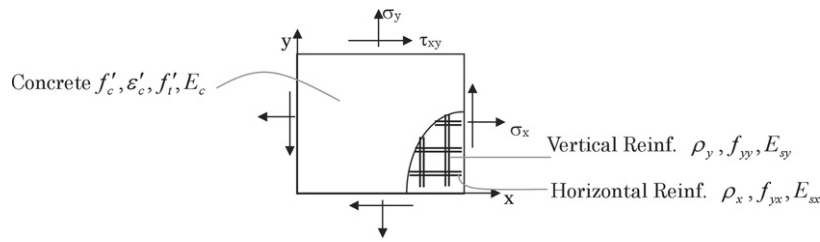
Fig. 1. A reinforced concrete membrane element subject to in-plane stresses.
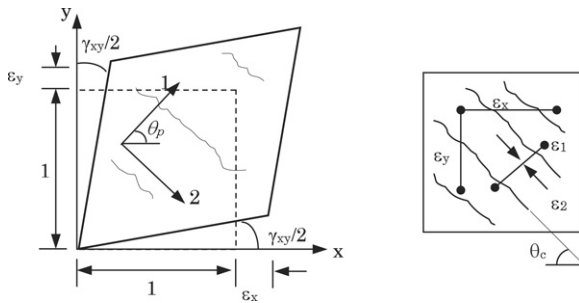

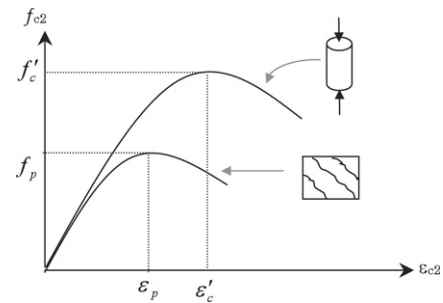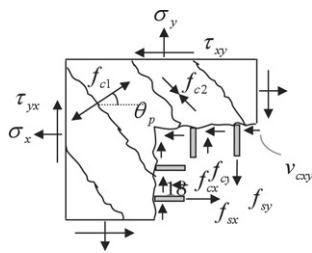Fig. 2. Average strains in concrete and reinforcements.

Fig. 3. A reinforced concrete in-plane shear element showing average stresses.

are satisfied by balancing the resultants of applied normal stresses (σ_x, σ_y, τ_{xy}) by resultants of the average concrete stresses (f_{cx}, f_{cy}, v_{cxy}) and reinforcement stresses (f_{sx}, f_{sy}). Equilibrium of moments requires that applied shear stresses, τ_{xy}, are entirely resisted by average shear stresses in the concrete, v_{cxy}, (ignoring the effect of reinforcement dowel action). Considering the free body diagram of the membrane element, in Fig. 3, equilibrium relationships for average stresses can be summarized as follows:

$$
\begin{aligned}
\sigma_x &= f_{cx} + \rho_x \cdot f_{sx} \\
\sigma_y &= f_{cy} + \rho_y \cdot f_{sy} \\
\tau_{xy} &= v_{cxy}
\end{aligned}
\tag{3}
$$

where, σ_x = total stress in x direction, σ_y = total stress in y direction, $\tau_{xy} = \tau_{yx}$ = shear stress, f_{cx} = concrete stress in x-direction, f_{cy} = concrete stress in y-direction, $v_{cxy} = v_{cyx}$ = concrete shear stress relative to x and y axes, f_{sx} = average reinforcement stress in x-direction, f_{sy} = average reinforcement stress in y-direction, ρ_{sx} and ρ_{sy} are the reinforcement ratios in x and y directions, respectively.

1.3. Constitutive laws

The constitutive laws for cracked reinforced concrete were derived from experimental studies on panel elements subjected

Fig. 4. A constitutive law for concrete in principal compression direction.

to in-plane stress conditions using the Panel Element Tester at the University of Toronto [5,14]. The test results were analyzed to develop constitutive models for cracked concrete in compression and tension. It was found that cracking of concrete resulted in degradation of strength, stiffness and ductility of concrete in compression. Fig. 4 illustrates the constitutive law for concrete in the principal compression direction, as applied in modified compression field theory.

$$
\begin{aligned}
f_P &= \beta f_c' \\
\varepsilon_p &= \beta \varepsilon_c' \\
\beta &= \frac{1}{1 + C_s C_d} \leqslant 1.0
\end{aligned}
\tag{4}
$$

where β is compression softening factor, C_d is a factor defined in terms of concrete tensile and compression strains, and C_s accounts for the influence of slippage on the cracks.

The concrete tension stiffening constitutive relationship applied in Modified Compression Field Theory is depicted in Fig. 5. The concrete tensile stress–strain relationship is linear prior to cracking of the concrete. After cracking, average concrete tensile stress is declining based on Eq. (5).

$$
f_t = \frac{f_t'}{1 + \sqrt{c_t \varepsilon_1}}
\tag{5}
$$

where, $f_t' = 0.33\sqrt{f_c'}$ (MPa) and $c_t = 2.2m$ where m is a factor in terms of the reinforcement ratio and the rebar diameter [13].

The VecTor2 default hysteresis model for concrete is the Nonlinear Plastic Offsets model proposed by Vecchio; for reinforcements, the Seckin Model (Bauschinger) is used [15].

2. WCOMD and smeared fixed crack concept

Program UC-win/WCOMD is an analytical tool for path-dependent two-dimensional static and dynamic nonlinear analysis of reinforced concrete structures (FORUM8 2003),
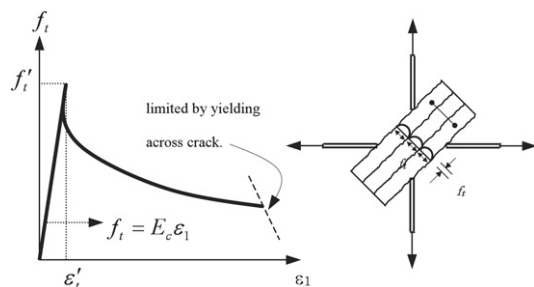
Fig. 5. Average stress–strain relationship for cracked concrete in tension.

based on a smeared reinforcement and smeared fixed crack approach with average strain-stress relationships for in-plane shear elements [6]. The program has two components: an analysis solver program and an interface program. The solver program was developed in the Concrete Laboratory, University of Tokyo, and deals primarily with two-dimensional nonlinear dynamic/static analysis of reinforced concrete structures. The interface program is a Windows based program developed by FORUM8 for mesh editing and configuration. In this study, the advanced mode of the program was selected to achieve the maximum possible damage states estimated by the program.

In the fixed crack model, when the principal stress reaches the concrete tensile strength, a crack develops perpendicular to the principal tensile stress direction. However, the crack orientation does not change during successive loading. The early fixed crack method had numerical problems caused by singularity of the material stiffness matrix. In addition, the crack pattern predicted by such an analysis lacks correlation with that observed in experiments [7]. Later, in order to overcome this problem, a cracked shear modulus was developed for the method to eliminate most of the numerical difficulties and numerical instability and to improve the accuracy of predicted results. Here, the current version of a fixed crack approach is briefly described.

2.1. Equilibrium and compatibility conditions

In the fixed crack method, a reinforced concrete element with multiple cracks with different orientations is formulated by applying nonlinear mechanisms for cracked concrete and elastic mechanisms for uncracked concrete. Equilibrium and compatibility conditions are satisfied simultaneously for cracked and uncracked concrete which lead to a secant stiffness matrix in the stress–strain field [6].

In this method, superposition of concrete average stress and reinforcement average stress gives the total average stress for a reinforced concrete element [8].

$$\{\sigma\}_{rc} = \{\sigma\}_c + \{\sigma\}_r \tag{6}$$

where $\{\sigma\}_{rc}$, $\{\sigma\}_c$, and $\{\sigma\}_r$ are stresses in the reinforced concrete, cracked concrete and reinforcement, respectively. The total average strain of a reinforced concrete element is obtained from the summation of strains caused by all cracks in the element and the uncracked concrete as

$$\{\varepsilon\} = \{\varepsilon\}_{c0} + \{\varepsilon\}_{c1} + \{\varepsilon\}_{c2} + \cdots + \{\varepsilon\}_{cn} \tag{7}$$

where $\{\varepsilon\}_{c0}$ is the uncracked concrete strain and $\{\varepsilon\}_{ci}$ is the strain due to crack in the i direction.

2.2. Active crack approach

The active crack method is a simplified but reasonably accurate method that allows the explicit derivation of the stiffness matrix without iterative computation [6]. This method was developed based on the fact that not all cracks in a multi-cracked element play a dominant role in element nonlinearity at the same time. In other words, a few cracks, called active cracks, are considered as dominant cracks and control the overall nonlinearity of the entire element. As a result, a much more simplified computational process is implemented for nonlinear analysis. This is one of the basic hypotheses of the WCOMD program.

2.3. Constitutive laws

Concrete before cracking is treated by the elasto-plastic fracture (EPF) model. The model idealizes uncracked concrete by combining plasticity, for residual deformation, and continuum fracture, for loss of elastic strain energy absorption. In the model, several microelements are connected in parallel. Each microelement is composed of an elastic spring, to represent the internal stress-bearing mechanism and energy absorption capacity, and a slider, for residual plastic deformation, connected in a serial chain. An idealization of the FPF model is depicted in Fig. 6.

For a cracked concrete element, anisotropic behaviour is modeled in the direction of the crack. The same uncracked concrete EPF model is applied for cracked concrete in compression. However, for cracked concrete, the compressive normal stress parallel with the crack direction is assumed uniaxial. Furthermore, compression strength degradation due to the damage caused by tensile strain is considered by applying a strength reduction factor. Concrete in tension follows the constitutive law of the EPF model until cracking. After the concrete cracks, a tension stiffening model, shown in Fig. 7, controls concrete tensile behaviour perpendicular to the cracks. A coupled compression-tension path-dependent model is used to compute the normal stress in concrete subjected to an alternate tension-compression loading path [6]. For reinforcement, a multi-surface plasticity model, proposed by Fukuura and Maekawa [6], is implemented to represent the nonlinear stress–strain hysteretic response. The shear stress and strain at the crack plane normal to the maximum principal stress direction are assumed to be zero at the moment of cracking. However, as loading proceeds, the principal axes of stress and strain rotate. Hence, the existing crack is no longer normal to the new principal direction. Therefore, in the fixed crack approach, a shear transfer model is applied for the cracked concrete based on the contact density theory [6].

3. Axial-shear-flexure interaction approach

The Axial-Shear-Flexure Interaction (ASFI) method [3] is a macro-model-based approach for displacement-based analysis
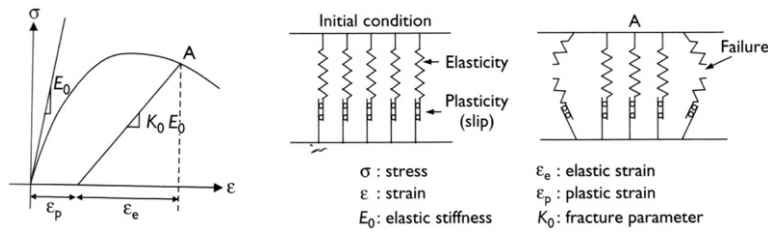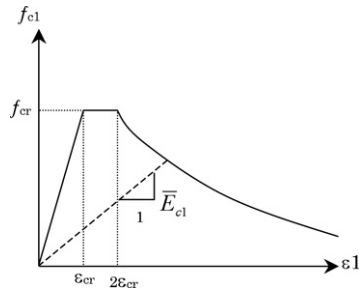
Fig. 6. The EPF elasto-plastic fracture model.

Fig. 7. Average stress–strain relationship for cracked concrete in tension.

Fig. 8. Average centroidal strain due to flexure to be contributed in the in-plane shear element.

of reinforced concrete columns and beams, comprising the three mechanisms of axial, shear and flexure. The axial-flexural mechanism is modeled by two adjacent flexure sections, and the axial-shear mechanism is modeled by a shear model between the two flexure sections. The total lateral drift of a column (γ) between two flexure sections is considered equal to the summation of the shear strain γ_s and the flexural drift ratio γ_f, between the two sections. Furthermore, the total axial strain of the column between the two sections, ε_x, is obtained from the summation of axial strains due to axial ε_{xa}, shear ε_{xs} and flexural ε_{xf} mechanisms.

$$\gamma = \gamma_s + \gamma_f$$
$$\varepsilon_x = \varepsilon_{xs} + \varepsilon_{xf} + \varepsilon_{xa}. \tag{8}$$

Flexure section analysis gives the axial strain caused by axial and flexural mechanisms, $\varepsilon_{xc} = \varepsilon_{xaf} + \varepsilon_{xf}$. On the other hand the axial-shear model gives axial strain due to axial and shear mechanisms, $\varepsilon_s = \varepsilon_{xas} + \varepsilon_{xs}$. Therefore, to obtain ε_x in Eq. (8), it is necessary to extract ε_{xf} from the section analysis, or to determine ε_{xs} from the shear model.

Assuming a linear strain relationship between two flexural sections of a column, as shown in Fig. 8, axial strain due to flexure between the two sections, ε_{xf}, is determined based on the relative centroidal deformation between the two sections by means of integration as Eq. (9).

$$\varepsilon_{xf} = \frac{1}{\ell_{12}} \int_0^{\ell_{12}} (\varepsilon_{xc1} - \varepsilon_{xc2}) \frac{x}{\ell_{12}} dx = 0.5(\varepsilon_{xc1} - \varepsilon_{xc2}) \tag{9}$$

where, ε_{xc1} and ε_{xc2} are the centroidal strains of two adjacent flexural sections and ℓ_{12} is the distance between the two sections. In the simplified ASFI method with one flexure section, a nonlinear centroidal strain distribution can be applied between the end section and inflection point.

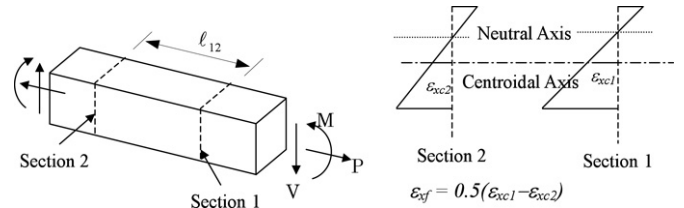Compatibility of axial deformations is satisfied when axial deformations due to axial mechanisms in the axial-shear element, ε_{xas}, and the axial-flexure element, ε_{xaf}, become identical.

$$\varepsilon_{xa} = \varepsilon_{xas} = \varepsilon_{xaf}. \tag{10}$$

For equilibrium, axial stress in the axial-flexure element, σ_{xf}, should be equal to axial stress in the axial-shear model, σ_{xs}. In addition, equilibrium of shear stress in the axial-flexure element, τ_f, and shear stress in the axial-shear model, τ_s, is satisfied simultaneously through the analysis.

$$\sigma_{xf} = \sigma_{xs} = \sigma_o$$
$$\tau_f = \tau_s = \tau \tag{11}$$

where σ_o is the applied axial stress determined by Eq. (12), and τ is the resultant shear stress. Shear stress in the axial-flexure mechanism, τ_f, and shear stress in the axial-shear mechanism, τ_s, are calculated by Eqs. (13) and (14), respectively.

$$\sigma_o = \frac{P}{BH} \tag{12}$$
$$\tau_f = \frac{M}{B d_f L_{in}} \tag{13}$$
$$\tau_s = \frac{V}{B d_s} \tag{14}$$

where P = applied axial load, H = depth of the section, B = width of the section, M = moment at the flexure section, L_{in} = distance between the flexure section and the inflection point, d_f = flexure depth of the section, d = effective depth of the section, V = the applied lateral load, and d_s = shear depth of the section.

Stresses in the directions perpendicular to the longitudinal axis of the column, the clamping stresses σ_y and σ_z, are ignored due to equilibrium between confinement pressure and hoop stresses.
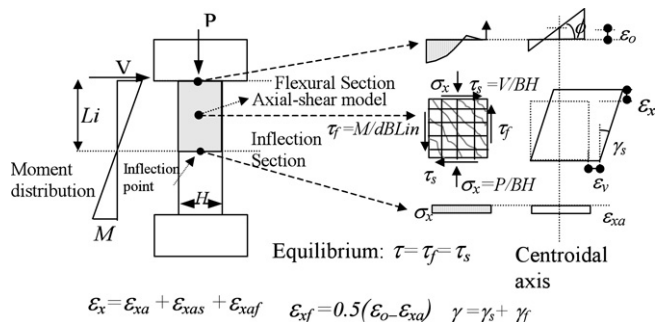
$$\sigma_y = \sigma_z = 0. \tag{15}$$

Fig. 9 shows the simplified ASFI method, for a reinforced concrete column, including equilibrium and compatibility

Table 1
Material property of the specimens

Speciemn	Type	B (mm)	H (mm)	$2L_{in}$ (mm)	S_h (mm)	ρ_g (%)	ρ_w (%)	f_{yx} (MPa)	f_{yy} (MPa)	f'_c (MPa)	P (kN)
No. 12	DC	300	300	900	150	2.26	0.14	415	410	28	540
No. 14	DC	300	300	900	50	2.26	0.43	415	410	26	540
No. 15	DC	300	300	900	50	2.26	0.85	415	410	26	540
No. 16	DC	300	300	600	50	1.8	0.43	415	410	27	540

DC = double curvature, or with two fixed ends, B = width of the section, H = Depth of the section, L_{in} = length of the column from the inflection point to the end section, S_h = hoop spacing, ρ_g = longitudinal reinforcement ratio, ρ_w = transverse reinforcement ratio, f_{yx} = longitudinal reinforcement yield stress, f_{yy} = transverse reinforcement yield stress, f'_c = concrete compression strength, and P = axial load.

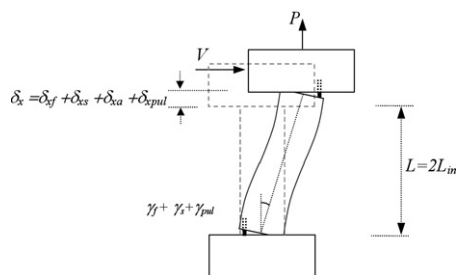Fig. 9. Axial-shear-flexure interactions in ASFI method.

Fig. 10. Axial and shear deformations of a column considered by ASFI method.

conditions. Total axial deformation of the column equals the axial strain developed by axial, shear, flexure and pullout mechanisms, and the total drift ratio equals the summation of shear, flexure and pullout deformations, as shown in Fig. 10. Constitutive laws for concrete and steel bars are considered to be the same as those in the MCFT. In addition, a pullout model is applied to consider the effect of pullout for tensile steel bars at the end-section of the columns [6].

The ASFI method was basically developed for displacement-based analysis of reinforced concrete columns and beams. Further study and development are required to enhance and assess the model for other types of elements such as shear walls [9].

4. Details of column specimens

Four column specimens, scaled to 1/3, representing columns located in the mid-frame of the first floor of a typical Japanese building with moderate height, tested previously [4], are selected for this study. Column specimens were loaded under constant axial load and static cyclic unidirectional lateral load. Details and material properties of the column specimens are

given in Table 1. The load set-up for a specimen, with height of 90 cm, is illustrated in Fig. 11.

All the specimens were subjected to a constant axial load of 540 kN, applied by two vertical jacks at the two sides of each column. At each loading step, axial loads from the two vertical jacks, and the corresponding vertical deformations, were controlled to ensure a uniform axial load on the columns section and to avoid any rotation at the two ends. The specimen's cyclic lateral loadings were controlled based on displacement. For lateral loading of specimens No. 12, No. 14, and No. 15, cyclic peak drift ratios (i.e. the column top horizontal displacement divided by the height of the column) $\pm 8/800$, $\pm 15/800$, $\pm 28/800$ were imposed and then monotonically increasing load was applied until axial failure. For specimen No. 16, peak drift ratios were $\pm 8/800$, $\pm 32/800$, followed by monotonically increasing load until complete loss of load capacity.

Column specimens No. 12, No. 14, and No. 15 were designed with almost identical characteristics except for transverse reinforcement ratios, to simulate different failure modes: shear, shear-flexure and flexure failures. However, column specimen No. 16 was shorter, compared to the other three columns, to simulate a short column at the location of wing-walls.

Based on experimental results, specimen No. 12, with the lowest transverse reinforcement ratios, failed in shear with a clear dominant shear crack on its face. A flexure response was exhibited by specimen No. 15 up to about 3.5% drift ratio, followed by shear failure [9]. Column No. 14 first failed in bond-flexure and then, with spreading shear and bond cracks on its face, failed in shear. Finally, column No. 16, the shortest specimen, failed in shear-compression just before reaching its flexure load capacity. Fig. 12 illustrates crack patterns and failures for specimens No. 12 to No. 15 soon after shear failure, in the post-peak stage.

5. Nonlinear analysis of the column specimens

Here, the analytical and modeling processes and results for column specimens are presented, as derived from the VecTor2 and WCOMD programs and the ASFI approach.

5.1. Implementation of VecTor2

The VecTor2 solver is equipped with a graphics-based preprocessor (FormWorks) to generate the finite element mesh. It includes facilities for data visualization and input, bandwidth
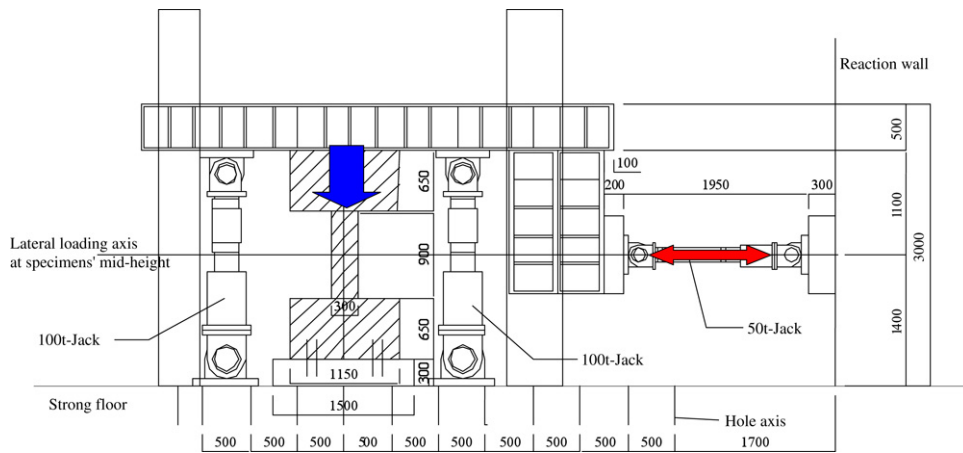
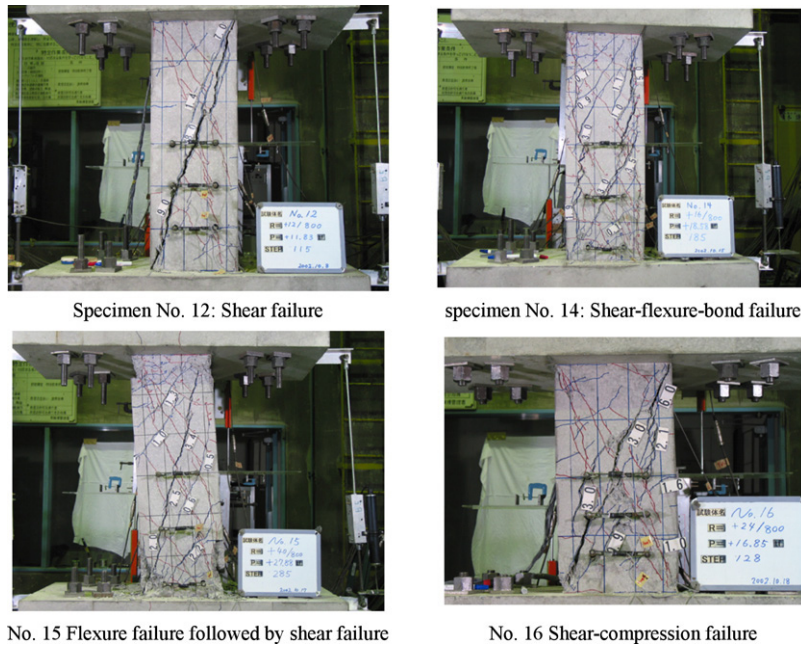Fig. 11. Loading apparatus and details of test setup in the experimental study.

Fig. 12. Crack patterns and failure modes of the reinforced concrete column specimens.

reduction and automatic mesh generation. Fig. 13-a shows the editor of FormWorks with a mesh generated for specimen No. 16.

The test setup for columns was simulated by considering two nearly rigid top and bottom stubs. Loading positions and support conditions for specimen No. 16 are illustrated in Fig. 13-b. Cover concrete was configured as unconfined concrete elements and core concrete was modeled as confined concrete elements. The dark (red) elements in the bottom and top stubs, shown in Fig. 13-b, were modeled as highly rigid to provide a zone without rotation.
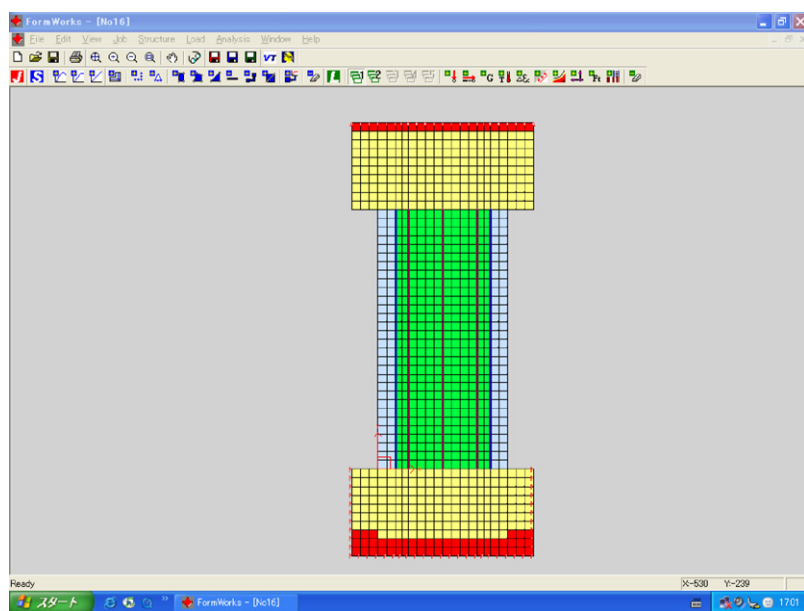
Nonlinear analyses were implemented via the VecTor2 program for the four reinforced concrete column specimens subjected to applied loads. Fig. 14 illustrates analytical and experimental results for the specimens. Furthermore, the ultimate load capacity, ultimate deformation capacity, pre-peak stiffness and post-peak stiffness, illustrated in Fig. 15,

were derived from the results by means of average values and outcomes were examined and compared in Table 2. Both Fig. 14 and Table 2 clearly indicate very good pre-peak correlations between the test and analysis for the columns. Strong correlations in post-peak responses were also achieved for specimens No. 12 and No. 16.
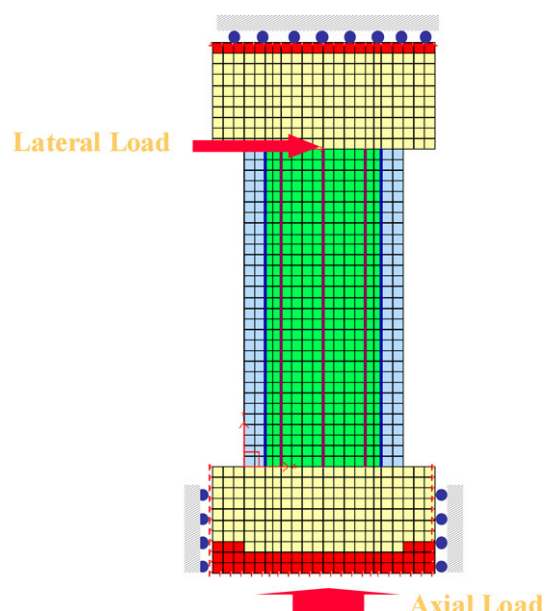
5.2. Modeling of reinforced concrete columns by WCOMD

Fig. 16 shows the editor of WCOMD and the mesh for one of the reinforced concrete column specimens generated for the analysis. Two joint elements were introduced in the top and bottom sections of each column to model the pullout effects of the specimen.

The concrete core was separated into two layers, in a direction perpendicular to the column plane. Then an in-plane shear element and overlapping plane element were applied for

(a) Editor of FormWorks.

(b) Loading positions and supports conditions for specimen No. 16.

Fig. 13. A reinforced concrete column configured in Form Works of VecTor2 program. (For interpretation of the references to colour in this figure legend, the reader is referred to the web version of this article.)

Table 2
Comparison of experimental and analytical results for specimen No. 12

Specimen	Results	Test	VecTor2		WCOMD		ASFI	
			Analysis	Analysis/Test	Analysis	Analysis/Test	Analysis	Analysis/Test
No. 12	UL (kN)	256	252	0.98	267	1.04	262	1.02
	UD (mm)	4.5	4.0	0.89	6.0	1.33	4.5	1.00
	E (N/mm)	79 000	85 000	1.08	66 000	0.84	79 500	1.01
	E_p (N/mm)	18 000	17 500	0.97	–	–	18 500	1.03
No. 14	UL (kN)	300	303	1.01	297	0.99	305	1.02
	UD (mm)	9	13	1.44[a]	8	0.89	12.4	1.38[a]
	E (N/mm)	67 000	66 500	0.99	66 500	0.99	67 000	1.00
	E_p (N/mm)	4 000	–	–	–	–	4 100	1.02
No. 15	UL (kN)	339	346	1.02	340	1.00	341	1.01
	UD (mm)	31.5	33	1.05	32	1.02	30	0.95
	E (N/mm)	59 000	58 500	0.99	55 000	0.93	58 500	0.99
	E_p (N/mm)	2 400	–	–	–	–	2 450	1.02
No. 16	UL (kN)	348	360	1.03	344	0.99	348	1.00
	UD (mm)	6	5.7	0.95	6.2	1.03	5.9	0.98
	E (N/mm)	110 000	120 000	1.09	110 000	1.00	107 000	0.97
	E_p (N/mm)	12 000	11 500	0.96	–	–	13 000	1.08

[a] Bond failure was observed for No. 14 during the test however bond behavior was not modeled in the analysis. UL: Ave. ultimate load, UD: Ave. ultimate drift, E: Ave. pre-peak stiffness, E_p: Ave. post-peak stiffness (see Fig. 18).

the two layers with different reinforcement ratios corresponding to the position of longitudinal and transverse reinforcement. The same support conditions and loads, as shown in Fig. 13-b, were employed for reinforced concrete columns modeled by the WCOMD interface software.

The analytical process is implemented by the main solver which is provided in the same package with the pre- and post-processors but executed in individual windows. Fig. 17 and Table 2 show analytical results by the WCOMD and the test results for the column specimens, which indicate consistent correlations for the pre-peak responses. The program limited the post-peak analysis implementation based on the default

failure criteria and could not estimate the post-peak response up to the complete loss of load capacity.

As an alternative, an analysis was undertaken for specimen No. 15 subjected to a monotonic loading. In general, it is expected that a column will have less deformation capacity under cyclic load than when it is subjected to a monotonic load. However, interestingly, analysis by WCOMD shows a shear failure for No. 15 under monotonic loading and a flexure response under cyclic loading, as illustrated in Fig. 17. Based on an oral communications with Maekawa, it is believed that this is due to the concept of the fixed crack approach and it is expected that the same response, shear failure, might be achieved for
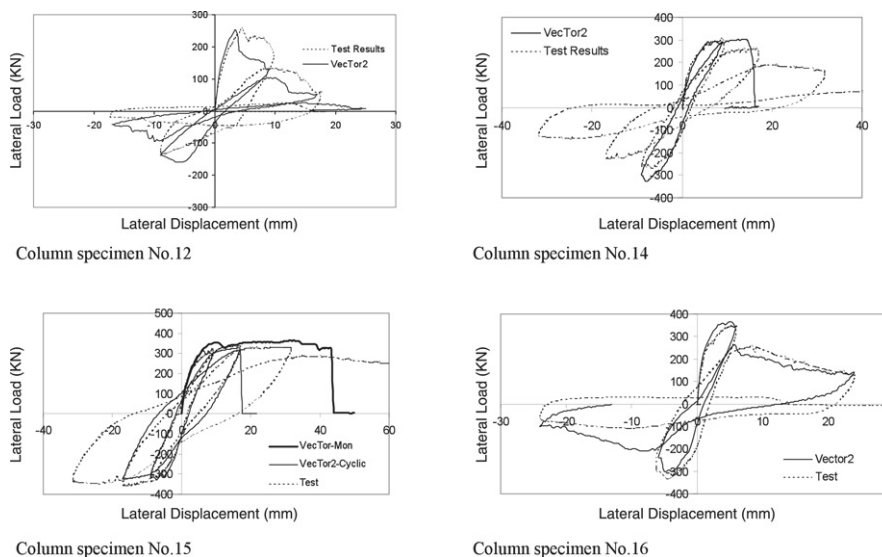
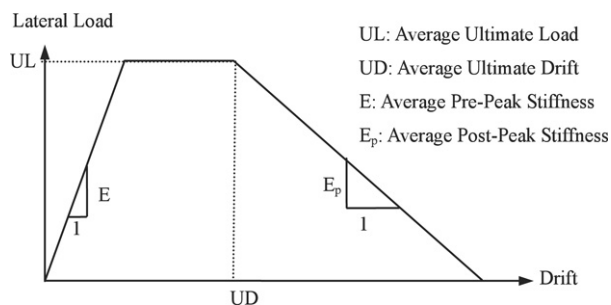Fig. 14. Analytical results by VecTor2 program comparing to the experimental outcomes.

Fig. 15. Illustration of terms and envelope curve for experimental results.

the specimen under a monotonic loading. However, no test data were available for the monotonic loading to verify this interesting result.

5.3. Analysis by ASFI method

Applying the simplified ASFI method, and by considering the symmetric conditions of the specimens, half of the columns' heights, from inflection point to one end, were modeled as shown in Fig. 9. A fiber model discretization was utilized for the end section as an axial-flexure model; conversely, a shear model was employed, as an axial-shear element, from the inflection point to the end section. For each column, a pushover analysis was implemented and a lateral load-drift ratio response was estimated. Results of the analysis by the ASFI method as well as experimental data are provided in Fig. 18 and Table 2 wherein the results of envelope curves for the FEM methods, obtained by VecTor2 and WCOMD (or UC-win) are also compared. In both Fig. 18 and Table 2, results of ASFI method show exceptionally good agreement with experimental values for both pre-peak and post-peak responses.

6. Discussion

As a result of this study, the first question that may come to mind is: which one of these two methods, fixed crack

or rotating crack, is more reliable for displacement-based analysis of reinforced concrete structures. A study on the latest developments on both VecTor2 and WCOMD programs will reveal that both approaches are implementing a hybrid method considering both fixed and rotating crack methodologies, which result in a reliable approach. In case of VecTor2, although the primary concept of the program is based on the rotating crack method and the Modified Compression Field Theory, an enhanced version of the program is based on a hybrid formulation combining elements of a fully rotating crack model and a fixed crack model; namely, the Disturbed Stress Field Model. Conversely, WCOMD originally was developed based on the fixed crack method; however, the last version of the program was modified based on an active crack approach. This conveys that both methods are based on a combination of rotating crack and fixed crack methods, however each method places heavier emphasis on its original methodology. Based on this study, results from both programs showed reasonable agreement with experimental data for pre-peak responses. Limited for the post-peak response based on failure criteria, WCOMD program provided post-peak results up to an average of 80% of the specimens' shear capacity. However, VecTor2 program gave strong results for post-peak response of the two column specimens critical in shear; No. 12, and No. 16, up to complete loss of shear capacity. WCOMD considers the pullout effect, due to slip of steel bars under tension stress at the section adjacent to the section with larger thickness, which results in a proper stiffness for the specimens. However, for specimen No. 12, results showed less stiffness compared to test data, as indicated in Table 2, possibly overestimating pullout deformation. Although, relatively similar response envelope curves were attained by VecTor2 for column No. 15 under lateral cyclic load and under lateral monotonic load, completely different responses were obtained by WCOMD for the specimen under the two loading conditions. This might be due to the conceptual fixed crack model used in the program. A larger number of elements is required to utilize a fine mesh on a
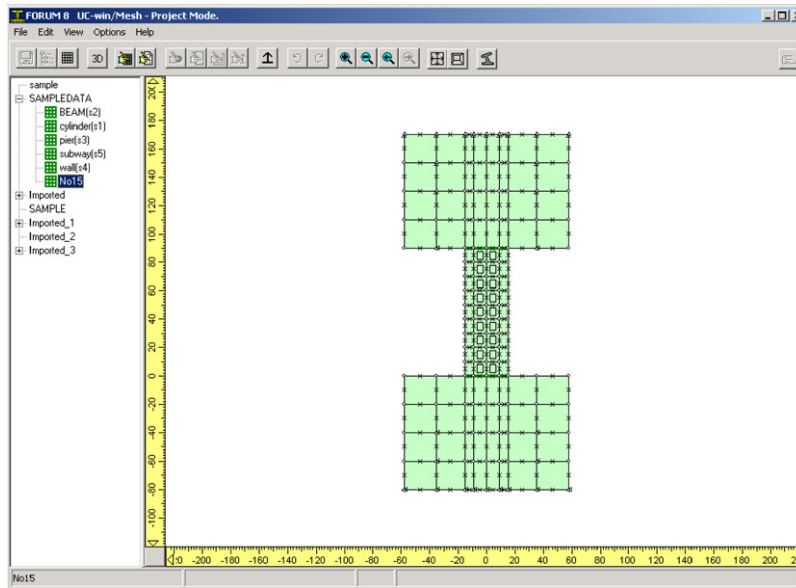
Fig. 16. A reinforced concrete column configured in WCOMD.

Column specimen No.12

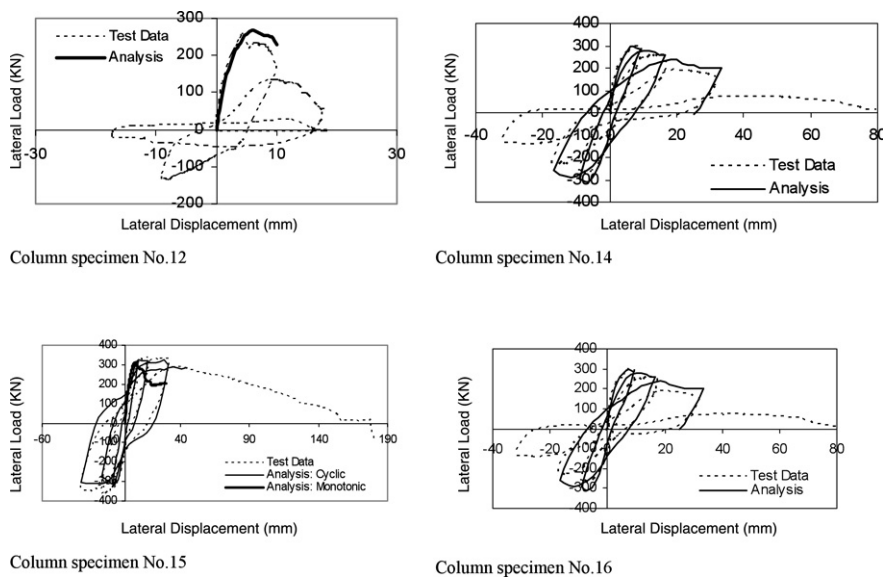Column specimen No.14

Column specimen No.15

Column specimen No.16

Fig. 17. Analytical results by WCOMD program comparing to the experimental outcomes.

structural domain by VecTor2 comparing to that by WCOMD. This is because rectangular elements with higher integration points are applied in WCOMD. This would reduce the time needed for an analysis by WCOMD program.

In the analysis by VecTor2, local failure of specimen No. 15 after ultimate drift prevented the program from attaining post-peak response. An attempt was made to estimate post-peak response of column No. 15 by VecTor2 program. To prevent premature failure in analysis, before complete loss of load capacity, domain of the column was utilized with larger size elements, comparing to the fine mesh applied for the specimen in Section 5.1. Although a higher load capacity for pre-peak response was obtained, a strong correlation was achieved for the post-peak response. This result suggests that by applying

a proper numerical method and appropriate element size, post-peak response might be achieved by the FEM method also for columns with dominant flexure behavior.

Comparing to the results obtained by the FEM methods, exceptionally good correlation was achieved by the ASFI method for both pre- and post-peak response. The Modified Compression Field Theory was found to be a powerful method for solving shear problems, when applied in the ASFI method to model the shear behavior. On the other hand, section analysis is a well accepted method for flexure problems, also employed in the ASFI method. Hence, coupling and interacting the two shear and flexure methods resulted in a proper analytical tool for nonlinear analysis of reinforced concrete columns, estimating the global behavior of the elements. The ASFI method was
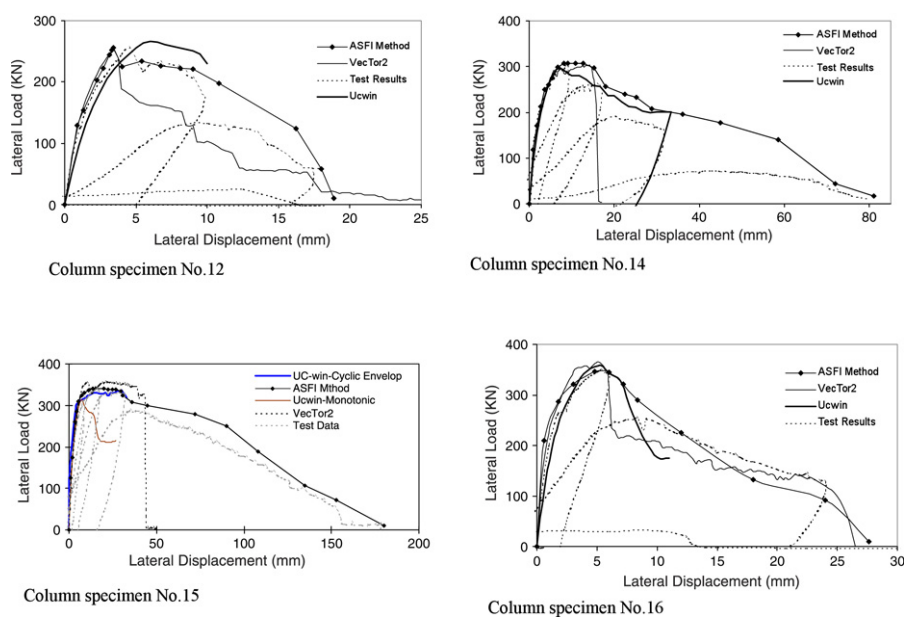
Fig. 18. Comparisons of experimental results and analytical outcomes of load-drift envelope curves for the specimens by ASFI, UC-win/WCOMD and VecTor2 programs.

easily implemented in Excel and few iterations were needed to achieve a proper convergence at each loading steps. Avoiding local failure modes, which were observed in the FEM analysis for columns No. 14 and No. 15, might be the main reason for the ASFI method being able to achieve strong post-peak response correlations with the test data for the column specimens.

7. Conclusions and recommendations

Overall, both FEM programs, VecTor2 and WCOMD, are powerful analytical tools in practice for the analysis of reinforced concrete elements up to their ultimate load state. In particular, VecTor2 software is highly reliable for displacement-based analysis of shear-critical problems, providing reliable results even for post-peak responses.

It is strongly expected that by applying a proper numerical solution technique in VecTor2, post-peak response can be attained for elements with dominant flexural behavior such as column No. 15.

Further experimental study is required to verify analytical results by WCOMD program for column No. 15 showing a shear failure under monotonic loading and a flexure response under cyclic loading. A clue might be found on the effects of crack opening and closure in the concept of fixed crack approach.

Analytical study by the Axial-Shear-Flexure method indicates that not only do the individual components of shear and flexure response play important roles in estimating reliable analytical results, but also their interactions with axial deformation have a significant effect on the response. Further simplification is recommended in ASFI method for application in practice for the purpose of performance-based design of reinforced concrete columns and beams as well as application to shear walls.

Practically, applicability of an FEM method is limited for nonlinear analysis of a large structure, such as a building.

This is because FEM methods would require excessively large amounts of memory and fastidious computation for such a structure. In this case, macroscopic models, such as the ASFI method, are proper analytical tools for nonlinear analysis of large building structures in practice.

Acknowledgement

References

[1] Rashid YR. Analysis of prestressed concrete pressure vessels. Nuclear Engineering and Design 1968;7(4):334–44.

[2] Cope RJ, Rao PV, Clark LA, Norris P. Modeling of reinforced concrete behavior for finite element analysis of bridge slabs. In: Taylor C, et al., editors. Numerical method for nonlinear problems 1. Swansea: Pineridge Press; 1980. p. 457–70.

[3] Mostafaei H, Kabeyasawa T. Axial-shear-flexure interaction approach for reinforced concrete columns. ACI Structural Journal 2007;104(2).

[4] Ousalem H, Kabeyasawa T, Tasai A, Iwamoto J. Effect of hysteretic reversals on lateral and axial capacities of reinforced concrete columns. Proceedings of the Japan Concrete Institute 2003;25(2):367–72.

[5] Vecchio FJ, Collins MP. The modified compression field theory for reinforced concrete elements subjected to shear. ACI Structural Journal 1986;83(2):219–31.

[6] Maekawa K, Pimanmas A, Okamura H. Nonlinear mechanics of reinforced concrete. London: Spon Press; 2003.

[7] Jain SC, Kennedy JB. Yield criterion for reinforced concrete slabs. Journal of Structural Division, ASCE 1974;100(ST3):631–44.

[8] Fukuura N, Maekawa K. Spatially averaged constitutive law for reinforced concrete in-plane elements with non-orthogonal cracking as far as 4-way directions. Journal of Materials, Concrete Structures and Pavements 1999; 45(634):177–95.

[9] Mostafaei H. Axial-shear-flexure interaction approach for displacement-based evaluation of reinforced concrete elements. Ph.D. dissertation. University of Tokyo, winter 2006.

[10] Vecchio FJ. Disturbed stress field model for reinforced concrete: Formulation. ASCE Journal of Structural Engineering 2000;126(8): 1070–7.

[11] Vecchio FJ. Disturbed stress field model for reinforced concrete: Implementation. ASCE Journal of Structural Engineering 2001;127(1): 12–20.

[12] Vecchio FJ, Lai D, Shim W, Ng J. Disturbed stress field model for reinforced concrete: Validation. ASCE Journal of Structural Engineering 2001;127(4):350–8.

[13] Bentz EC. Sectional analysis of reinforced concrete structures. Ph.D. thesis. Toronto: University of Toronto; 1999.

[14] Vecchio FJ, Collins MP. Compression response of cracked reinforced concrete. ASCE Journal of Structural Engineering 1993;119(12): 3590–610.

[15] Wong PS, Vecchio FJ. Vector2 & Formwork user's manual. Department of Civil Engineering, University of Toronto; 2002. 214 pp.